Analysis of a Near-Free-Floating Vibration Isolation Platform

Martin Regehr*

ABSTRACT. — Pointing control for deep-space lasercom is expected to be challenging because, for the apertures and wavelengths contemplated (of order 20 cm and 1 μm, respectively), the width of the beam transmitting data to Earth will be of order a few microradians. To address this challenge, JPL and others have been developing a vibration isolation system in which the lasercom telescope is nearly free-floating next to the spacecraft, being physically connected to the spacecraft only by a set of flexible wires and fibers referred to as an umbilical. The telescope's position relative to the spacecraft is sensed by noncontact sensors and the telescope is controlled by noncontact (voice coil) actuators. The telescope pointing error, relative to Earth, is also sensed by a pointing detector in the telescope, which images an Earth-based laser beacon. The telescope moves in six degrees of freedom, of which two (pitch and yaw) are the pointing of the telescope, and are of principal importance. This article describes a controller for controlling the telescope, and a simplified method of analyzing the closed-loop behavior of the system. Several mechanisms for cross-coupling between the degrees of freedom are present, including off-diagonal elements in the umbilical spring constant matrix, and the telescope having significant products of inertia; as a result, the dynamics of the closed-loop system are described by a full 6×6 transfer matrix. Approximations that take into account only one or two cross-coupling mechanisms at a time, however, and which result in block-diagonal models for the system, provide excellent agreement with the full model. These approximations provide insight useful for designing the controller, and numerical models indicate that a controller designed using these approximations provides performance that meets pointing requirements.

I. Introduction

Precise pointing control is generally required for laser communications (lasercom), and particularly for lasercom terminals with large apertures: The beam transmitted from a 20-cm aperture may have a beam divergence of only a few microradians, and may require submicroradian pointing control to avoid unacceptable link loss. To provide precision pointing, JPL [1] and others [2–7] have been developing nearly free-floating vibration isolation systems. Figure 1 shows the JPL system controlling a platform containing a lasercom telescope.

* Guidance and Control Section, retired.

The research described in this publication was carried out by the Jet Propulsion Laboratory, California Institute of Technology, under a contract with the National Aeronautics and Space Administration.

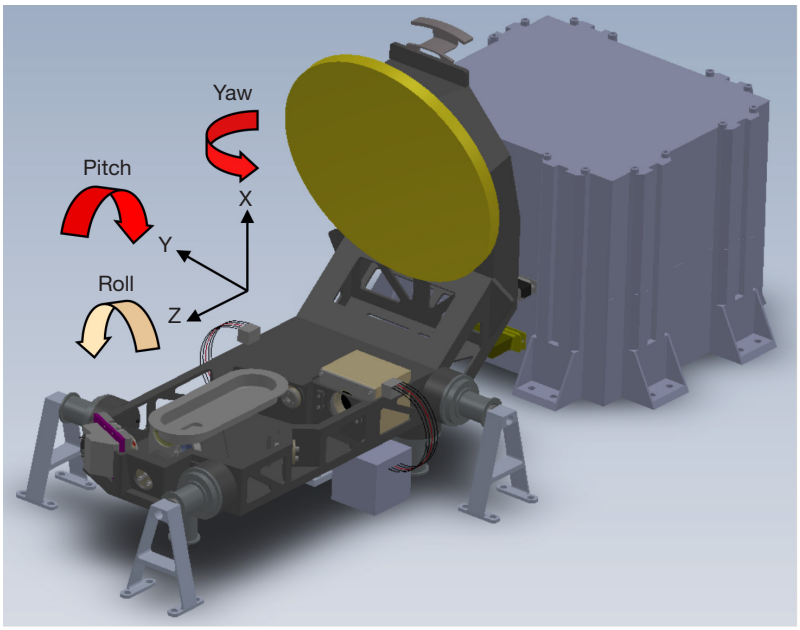

Figure 1. Platform configuration.

The system isolates the platform from spacecraft disturbances, providing a stable, steerable platform. The platform is physically connected to the spacecraft only by a set of flexible wires and fibers, referred to collectively as the umbilical, that supply electrical and optical power to the platform, and that provide two-way data communications. Six noncontact relative sensors sense the position and attitude of the platform relative to the spacecraft, and six noncontact voice coil actuators control the platform's position and attitude. A pointing detector on the platform, which images a ground-based beacon, senses the attitude of the platform in two degrees of freedom, pitch and yaw, with respect to line of sight to Earth.

This article describes an approach for analyzing the pointing performance of the platform, generalizing an approach by Pedreiro [8] to the case in which the umbilical stiffness is not negligible. It presents expressions for finding the spring constant matrix of the umbilical, given the characteristics of each of the strands in the umbilical, and derives equations of motion, which, when solved, produce transfer functions from motion of the spacecraft interface (the point on the spacecraft at which the platform is attached) to platform pointing errors. It also provides a summary of the principal mechanisms by which spacecraft interface motion causes pointing errors, and provides simple approximate analytical expressions for several of these mechanisms.

II. System Model

The vibration isolation system works by attenuating high-frequency spacecraft motion passively, relying on a very compliant physical connection between the spacecraft and the platform, and suppressing low-frequency motion actively, i.e., employing a control system to point the telescope at the ground beacon. Residual spacecraft disturbances and sensor noise are the principal sources of pointing error in the platform.

The control system controls the attitude of the platform using feedback from the relative sensors and from the pointing detector. For simplicity, the control configuration is assumed to be that shown in Figure 2. Two separate controllers are used: a controller with gain matrix G_E, feeding back from the pointing sensor, and a "local" controller with gain matrix G_L, feeding back from the relative sensors.

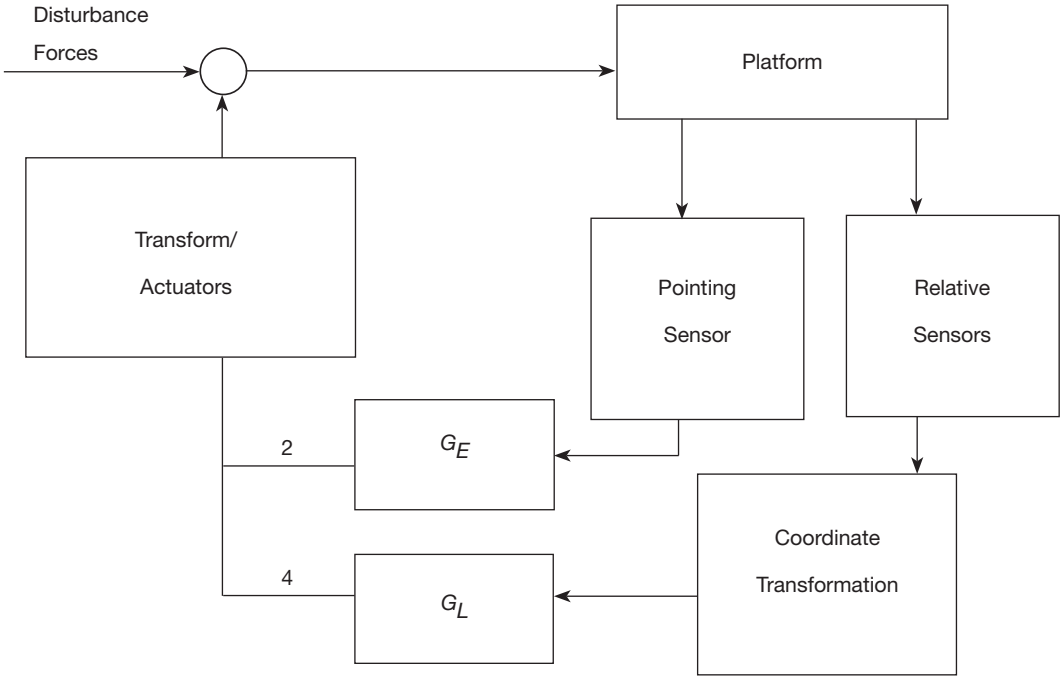

Figure 2. Controller configuration.

The pointing detector directly measures pitch and yaw, the pointing degrees of freedom, relative to the ground beacon; these pitch and yaw signals are processed by the controller G_E to provide pitch and yaw (torque) commands. We choose G_E to be diagonal, i.e., pitch errors sensed result only in pitch torque commands, and the same for yaw.

Each of the relative sensors in general measures a linear combination of the six degrees of freedom of the platform, relative to the spacecraft interface. A coordinate transformation is used to transform the sensor signals into the six principal degrees of freedom, i.e., X, Y, Z, yaw, pitch, and roll; of these, the four nonpointing degrees of freedom, X, Y, Z, and roll, are processed by the local controller G_L to provide translation (force) and roll (torque) commands. The pitch and yaw signals are discarded, and we also choose G_L to be diagonal.[1]

Torque commands from the controller G_E feeding back from the pointing sensor are combined with force and torque commands from the local controller G_L in a transformation matrix that calculates and drives the forces needed at the six voice coil actuators to produce the commanded forces and torques.

[1] Choosing diagonal controllers results in considerably simpler analysis than if we were to consider general controllers. As noted below, some performance improvements, perhaps significant, may be achievable by using different controllers.

To avoid burdening the spacecraft attitude control system (ACS), we assume that high-rate attitude estimates are not available from the ACS, although their availability could result in substantial performance improvements.

A. Equations of Motion

In this section, we find the equation of motion for calculating the transfer function from spacecraft interface motion to platform motion. We first define the six-dimensional vector $\vec{x}_s$ as the generalized position of the spacecraft interface, the first three elements of which are position (X, Y, and Z), and the remaining three of which are rotation (yaw, pitch, and roll). Similarly, $\vec{x}_p$ is the generalized position of the platform.

The equation of motion is the following six-dimensional vector equation, which equates the mass matrix times acceleration to forces from the umbilical, and from the controllers:[2]

$$-\omega^2 M\vec{x}_p = \left(K + j\omega c + G_L\right)\left(\vec{x}_s - \vec{x}_p\right) - G_E\vec{x}_p \tag{1}$$

where ω is the angular frequency, c is a 6×6 matrix of umbilical damping coefficients, and M is the mass matrix, which is a block diagonal matrix with the lower right 3×3 block containing the moments of inertia and the upper left block being diagonal with the diagonal elements equal to the mass of the platform.[3]

The matrix K is the 6×6 spring constant matrix of the umbilical, which acts as a spring, generating a force and torque on the platform proportional to its displacement, from its equilibrium position, relative to the spacecraft interface. This force may be written as

$$\vec{F}_{\text{Umbilical}} = K\left(\vec{x}_s - \vec{x}_p\right)$$

where $\vec{F}_{\text{Umbilical}}$ is a generalized force vector within which the first three elements are X, Y, and Z forces on the platform, and the remaining three elements are yaw, pitch, and roll torques.

Damping is expected to have negligible effects in virtually all situations, and we drop the damping term $j\omega c$ for the remainder of the analysis, to simplify the formulae. Collecting terms in $\vec{x}_s$ and $\vec{x}_p$ then yields:

$$\left(K + G_L + G_E - \omega^2 M\right)\vec{x}_p = \left(K + G_L\right)\vec{x}_s. \tag{2}$$

---

[2] This equation applies in an inertial, i.e., nonrotating, coordinate system.

[3] The following mass matrix was used here, obtained from a point design (in units of kg and kg m^2):

$$M = \begin{bmatrix} 3.5 & 0 & 0 & 0 & 0 & 0 \\ 0 & 3.5 & 0 & 0 & 0 & 0 \\ 0 & 0 & 3.5 & 0 & 0 & 0 \\ 0 & 0 & 0 & 0.083 & 0 & 0.03 \\ 0 & 0 & 0 & 0 & 0.106 & -0.003 \\ 0 & 0 & 0 & 0.03 & -0.003 & 0.043 \end{bmatrix}$$

This is readily inverted numerically, at any given frequency, to find the matrix of closed-loop transfer functions from motion of the spacecraft interface to motion of the platform. This transfer function matrix is defined as follows:

$$\vec{x}_p = H(\omega)\vec{x}_s$$

and it is given by

$$H(\omega) = \left(K + G_L + G_E - \omega^2 M\right)^{-1}\left(K + G_L\right). \tag{3}$$

The Umbilical Spring Constant Matrix

The umbilical consists of several strands, each in the form of a semicircle. The spring constant matrix for a strand may be calculated using a finite-element model or derived analytically.[4] Each element of the spring constant matrix is the force or torque that must be applied to one end of the strand for the strand to experience a unit displacement in the direction of, or a unit rotation about, a particular axis.

For the results obtained here, we use a matrix calculated using finite-element analysis of a bare glass fiber, curved into a semicircle with a diameter of 40 mm, and oriented as one of the strands shown in Figure 1, on the –Y side of the platform. The matrix is in units of mN/m for the upper left block (which gives the ratio of force to translation), mN/rad for the upper right block (force to rotation), mNm/m for the lower right block (torque to translation), and mNm/rad for the lower right block (torque to rotation):

$$K_{\text{strand}} = \begin{bmatrix} 43.81 & 0 & 0 & 0 & 0 & -1.12 \\ 0 & 8.30 & 0 & 0 & 0 & 0.33 \\ 0 & 0 & 6.30 & 0.17 & -0.25 & 0 \\ 0 & 0 & 0.17 & 0.011 & -0.0069 & 0 \\ 0 & 0 & -0.25 & -0.0069 & 0.016 & 0 \\ -1.12 & 0.33 & 0 & 0 & 0 & 0.048 \end{bmatrix}.$$

The spring constant matrix K used in Equation (1) differs from this not only because the umbilical contains multiple strands, but also because it is defined such that each of its elements is the force or torque experienced by the platform about its center of mass, resulting from displacement of the platform or rotation of the platform about its center of mass. Thus, for any umbilical strand that does not attach to the center of mass of the telescope, the spring constant matrix must be transformed accordingly. This transformation accounts for the fact that, for example, when the platform rotates about its center of mass, the end of the umbilical strand rotates and, in general, translates as well.

We derive the transformation needed to account for this difference as follows. For a lossless spring, the change in the energy V stored in the spring equals the work done on the spring, and the force and torque can be written as the gradient of the energy stored:

$$K_{ij} = \frac{\partial^2 V}{\partial x_i \partial x_j} \tag{4}$$

[4] N. Pedreiro, personal communication, May 11, 2011.

where x_1, x_2, x_3 are position coordinates and x_4, x_5, x_6 are angular coordinates.

In another coordinate system, denoted by primed indices, the spring constant matrix transforms as a covariant tensor,[5] i.e.,

$$\begin{aligned} K_{i'j'} &= \frac{\partial x_i}{\partial x_{i'}} \frac{\partial x_j}{\partial x_{j'}} \frac{\partial^2 V}{\partial x_i \partial x_j} \\ &= J_{i'i} K_{ij} J_{jj'} \\ &= J^T K J \end{aligned} \tag{5}$$

where summation over repeated indices is implied, and J, with elements $J_{ii'} = \frac{\partial x_i}{\partial x_{i'}}$, is the Jacobian of the transformation. We find two types of Jacobian, one for translations of the coordinate system, and one for rotations.

The Jacobian for translation is

$$J = \begin{bmatrix} I & \vec{R}\times \\ 0 & I \end{bmatrix} \tag{6}$$

where $\vec{R}$ is the vector representing the translation, and

$$\vec{R}\times \equiv \begin{bmatrix} 0 & -R_3 & R_2 \\ R_3 & 0 & -R_1 \\ -R_2 & R_1 & 0 \end{bmatrix}.$$

The Jacobian for a rotation is just the transformation itself:

$$J = \begin{bmatrix} Q & 0 \\ 0 & Q \end{bmatrix} \tag{7}$$

where Q is a 3×3 matrix representing the transformation between the coordinate systems.

These transformations are applied sequentially. For example, to calculate the contribution of one fiber on the –Y side of the platform to the total spring constant, we use Equation (5) with the Jacobian from Equation (6) to translate the spring constant matrix in the –Y direction, and in the +Z or –Z direction according to the particular position of the strand. The spring constant for the entire umbilical is then found by summing the contributions from all of the strands, each suitably transformed.

In the configuration of Figure 1, the umbilical has 10 strands, five on each side of the platform. One set of five attaches at X = 2 cm (i.e., 2 cm higher than the center of mass in Figure 1), and Y = –9 cm and with five different values of Z, separated in increments of 5 mm, centered on Z = 0. The other set of five attaches at a set of points also separated in increments of 5 mm, centered on the point X = 2 cm, Y = 9 cm, and Z = 0. When the spring constant matrix of each of these strands is transformed according to its position, and, for each strand at Y = 9 cm, to account for its rotation relative to the reference strand, and the resulting transformed matrices are summed, the total spring constant matrix for the umbilical is found to be (in the same units as those used for K_{strand}):

[5] See, for example, R. Adler, M. Bazin, and M. Schiffer, *Introduction to General Relativity*, p. 19, McGraw-Hill, 1965.

$$K = \begin{bmatrix} 438.1 & 0 & 0 & 0 & 0.13 & 1.13 \\ 0 & 83.0 & 0 & -0.025 & 0 & 5.0 \\ 0 & 0 & 63.0 & -0.16 & -3.78 & 0 \\ 0 & -0.025 & -0.16 & 0.31 & 0.0095 & -0.0015 \\ 0.13 & 0 & -3.78 & 0.0095 & 0.31 & 0 \\ 1.13 & 5.0 & 0 & -0.0015 & 0 & 2.19 \end{bmatrix}$$

Controllers

As mentioned above, we assume for simplicity that each of the two controllers G_L and G_E is diagonal, with transfer functions on the diagonal selected so that the loop shape, measured through each diagonal element, approximates an integrator.[6] This is accomplished by including in each of the controller transfer functions a pole at DC and two zeros at an angular frequency equal to the square of the ratio of the diagonal spring constant matrix element to the diagonal mass element, i.e.,

$$\omega_{zi} = \sqrt{\frac{K_{ii}}{M_{ii}}}.$$

Having gains that increase without limit, these controllers are not realizable, but it is believed, and consistent with numerical tests, that adding two poles well above the unity gain frequency of each controller results in realizable controllers and nearly unchanged system performance.

B. Disturbance Coupling Mechanisms

Various coupling mechanisms cause spacecraft motion to produce platform pointing errors, i.e., motion in pitch or yaw. We begin by considering a simplified, diagonal system, and then consider the effects of off-diagonal elements in the mass matrix and the spring constant matrix, and imperfections in the transformation matrices for the sensors and actuators.

Direct

If the mass matrix and the spring constant matrix were diagonal, and the transformation matrices were ideal, then the six degrees of freedom of the system would be uncoupled, i.e., the transfer function matrix would be diagonal, and only pitch or yaw motion of the spacecraft interface would produce pitch or yaw motion, respectively, of the platform. Using Equation (3), the yaw–yaw transfer function, for example, would be

$$H_{44} = \frac{K_{44}}{\left(K_{44} + G_{E44} - \omega^2 M_{44}\right)}.$$

At low frequencies, the gain term in the denominator dominates, and

[6] These simple controllers were found by P. Thompson of Systems Technology Inc., working under contract to JPL, to have mediocre stability margins. The addition of a lead to the roll control loop, to produce a small phase adjustment, was found to mitigate this problem; this change did not affect the other conclusions drawn here, and resulted in a small performance improvement.

$$H_{44} \cong \frac{K_{44}}{G_{E44}},$$

with disturbance suppression provided by active rejection, while at high frequencies

$$H_{44} \cong \frac{K_{44}}{-\omega^2 M_{44}},$$

with passive isolation providing suppression. The direct pitch transfer function is analogous:

$$H_{55} = \frac{K_{55}}{\left(K_{55} + G_{E55} - \omega^2 M_{55}\right)}.$$

These idealized direct transfer functions are a good approximation to the transfer functions calculated when all of the off-diagonal matrix elements of the system are included, as is explained below in the context of Figures 3 and 4.

We now turn to mechanisms that cause coupling from spacecraft interface motion in non-pointing degrees of freedom to platform pointing error. Three important mechanisms have been identified for such coupling. They are off-diagonal elements in the spring constant matrix, products of inertia, and imperfections in the transformation matrices for the sensors and actuators.

Coupling from Z to Pitch

The coupling from spacecraft interface motion in the Z direction to pitch pointing error is predominantly caused by off-diagonal elements in the umbilical spring constant matrix. The closed-loop transfer function from Z to pitch can be found analytically assuming that the off-diagonal spring constant term is the only off-diagonal element in the system. After reordering of the rows and columns, Equations (2) and (3) become block-diagonal with one 2×2 block and four 1×1 blocks. This system can be solved analytically to get

$$H_{53} \cong \frac{-K_{53} M_{33} \omega^2}{D_{53}}$$

with

$$\begin{aligned} D_{53} = & -K_{53}^2 + G_{E55} G_{L33} + G_{E55} K_{33} + G_{L33} K_{55} - G_{E55} M_{33} \omega^2 - G_{L33} M_{55} \omega^2 \\ & + K_{33} K_{55} - K_{33} M_{55} \omega^2 - K_{55} M_{33} \omega^2 + M_{33} M_{55} \omega^4. \end{aligned}$$

Approximation is indicated because this expression assumes all off-diagonal elements in the system except K_{53} and K_{35} are zero. Numerically, this result is in good agreement with the Z to pitch coupling observed in the full model, as discussed below in the context of Figure 4. We see from this expression that if the local gain is sufficiently large, spacecraft interface translation in Z will not result in pitch pointing error through this mechanism. This is because if the controller forces the platform to follow the spacecraft interface closely, the umbilical deforms little and does not exert significant forces or torques on the platform.

Coupling from Roll to Pitch and Yaw

At frequencies at which the roll controller gain is significant, the principal coupling from spacecraft interface roll to pitch and yaw is through the nonzero products of inertia of the platform, e.g., M_{46} and M_{56}.[7] As the controller endeavors to cause the platform to follow the spacecraft interface in roll, it exerts roll torques on the platform, which, through the products of inertia, become pointing errors. Solving the block-diagonal system with one 2×2 block and four 1×1 blocks results in the following approximate expression for the transfer function from roll to yaw:

$$H_{46} \cong \frac{M_{46}^2 \omega^4 \left(G_{L66} + K_{66}\right)}{D_{46}}$$

with

$$\begin{aligned} D_{46} = &-M_{46}^2 \omega^4 + G_{E44} G_{L66} + G_{E44} K_{66} - G_{E44} M_{66} \omega^2 - G_{L66} M_{44} \omega^2 \\ &+ K_{44} K_{66} - K_{66} M_{44} \omega^2 - K_{44} M_{66} \omega^2 + M_{66} M_{44} \omega^4. \end{aligned}$$

The transfer function from roll to pitch is analogous. These equations show, in the numerator, that the roll controller acts as a parallel force to the umbilical, producing potentially significant roll torques on the platform, which become pointing errors through the products of inertia. Reducing the roll controller gain reduces this effect, and this coupling mechanism limits the amount of roll gain that can be used.

Coupling from Y to Pitch and Yaw

The dominant coupling from Y to the pointing degrees of freedom arises through the combination of the spring constant matrix element K_{26}, which couples Y motion to roll torque, and the nonzero products of inertia of the platform, which couple roll torques into pointing errors. The transfer functions from Y to pitch or yaw can be derived analytically by solving a 6×6 system that is block diagonal with one 3×3 block and three 1×1 blocks.[8] Increasing the gain in the Y controller reduces this coupling by reducing the deformation of the umbilical.

---

[7] This effect could be attenuated by the use of a different controller, which might, for example, command platform rate instead of torque, as is done with spacecraft. This approach was not found to be necessary to meet requirements with this design, but might well lead to overall performance improvements.

[8] The analytic expression obtained by solving the system in the 3×3 block (using machine symbol manipulation) is:

$$H_{42} \cong \frac{K_{26} M_{22} M_{46} \omega^4}{D_{42}}$$

with

$$\begin{aligned} D_{42} = {} & G_{E44} K_{26}^2 + G_{L22} M_{46}^2 \omega^4 + K_{26}^2 K_{44} - K_{26}^2 M_{44} \omega^2 + K_{22} M_{46}^2 \omega^4 - M_{22} M_{46}^2 \omega^6 - G_{E44} G_{L66} G_{L22} \\ & - G_{E44} G_{L66} K_{22} - G_{E44} G_{L22} K_{66} - G_{L66} G_{L22} K_{44} + G_{E44} G_{L66} M_{22} \omega^2 + G_{E44} G_{L22} M_{66} \omega^2 \\ & + G_{L66} G_{L22} M_{44} \omega^2 - G_{E44} K_{22} K_{66} - G_{L66} K_{22} K_{44} - G_{L22} K_{44} K_{66} + G_{E44} K_{22} M_{66} \omega^2 \\ & + G_{E44} K_{66} M_{22} \omega^2 + G_{L66} K_{22} M_{44} \omega^2 + G_{L66} K_{44} M_{22} \omega^2 + G_{L22} K_{44} M_{66} \omega^2 \\ & + G_{L22} K_{66} M_{44} \omega^2 - K_{22} K_{44} K_{66} - G_{E44} M_{22} M_{66} \omega^4 - G_{L66} M_{22} M_{44} \omega^4 \\ & - G_{L22} M_{44} M_{66} \omega^4 + K_{22} K_{44} M_{66} \omega^2 + K_{22} K_{66} M_{44} \omega^2 + K_{44} K_{66} M_{22} \omega^2 \\ & - K_{22} M_{44} M_{66} \omega^4 - K_{44} M_{22} M_{66} \omega^4 - K_{66} M_{22} M_{44} \omega^4 + M_{22} M_{44} M_{66} \omega^6. \end{aligned}$$

This expression is cumbersome and appears to offer little insight, but is readily evaluated numerically to validate the approximation.

Imperfect Actuator or Sensor Transformation

Because of imperfections in the actuator and sensor transformation matrices, a sensed error in one degree of freedom, or a command in one degree of freedom, will result in forces and torques in other degrees of freedom. To analyze the resulting coupling from Z motion to pitch pointing error, for example, we model this by assuming that when a Z force is commanded, a pitch torque of 1 mm times the commanded force is applied. Again by solving a block diagonal system with a 2×2 block containing this off-diagonal actuation term, we get

$$H_{53} \cong \frac{-rG_{L33}M_{33}\omega^2}{\left(G_{E55} + K_{55} - M_{55}\omega^2\right)\left(G_{L33} + K_{33} - M33\omega^2\right)}$$

where r is the factor, in this case 1 mm, representing the degree of imperfection of the transformation matrices. This may correspond, for example, to a 1 percent error in the proportion in which two voice coils, separated by 10 cm, are driven.

Comparing to direct coupling, we see that this mechanism will degrade the pointing performance by a factor of

$$\frac{rG_{L33}M_{33}\omega^2}{K_{55}}$$

if G_{L33} is the largest of the three terms in the factor $(G_{L33} + K_{33} - M_{33}\omega^2)$, and by a factor of

$$\frac{rG_{L33}}{K_{55}}$$

if $M_{33}\omega^2$ is the largest of these three terms. Reducing the local gain reduces this coupling.

Comparison Between Full and Approximate Transfer Functions

Figures 3 and 4 show the numerically calculated closed-loop transfer functions from spacecraft interface motion to platform pointing error, and approximate expression for the transfer function elements that are dominant, such as coupling from yaw to yaw, from roll to yaw, and from Z to pitch. Perfect transformation matrices are assumed. The agreement between the approximate transfer functions, which approximate the full 6×6 system with a block diagonal system as described above, is quite good, making it possible to use this understanding of the principal coupling mechanisms to guide design decisions.

Figure 5 shows the transfer functions to pitch when a 1 mm imperfection in the Z drive transformation is assumed. Comparing Figure 4 and Figure 5, we see the increase in coupling from Z to pitch at frequencies above 0.1 Hz, where this mechanism dominates.

C. Noise

To assess the effects of sensor noise on pointing performance, we rewrite the equations of motion, setting to zero the spacecraft interface motion, and adding terms corresponding to forces applied to the platform by the two controllers as a result of noise at their inputs:

$$-\omega^2 M\vec{x}_p = \left(K + G_L\right)\left(-\vec{x}_p\right) - G_E\vec{x}_p + G_L\vec{x}_{nL} + G_E\vec{x}_{nE}.$$

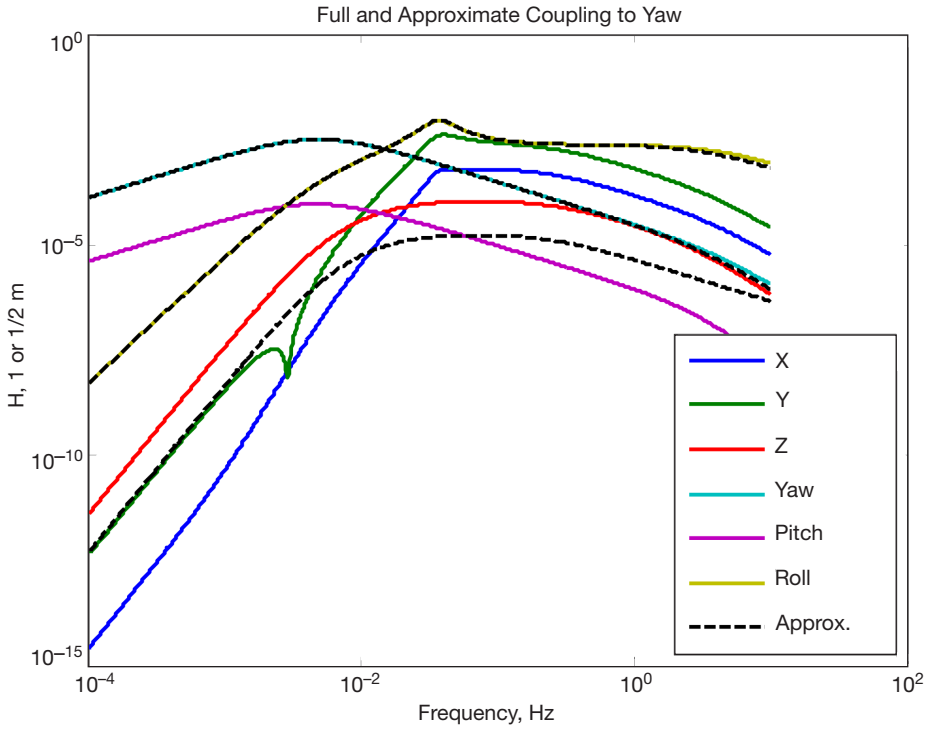

Figure 3. Transfer functions (magnitude) from spacecraft interface motion to platform yaw, calculated using the full 6 × 6 equation of motion and ("Approx.") using block-diagonal approximations.

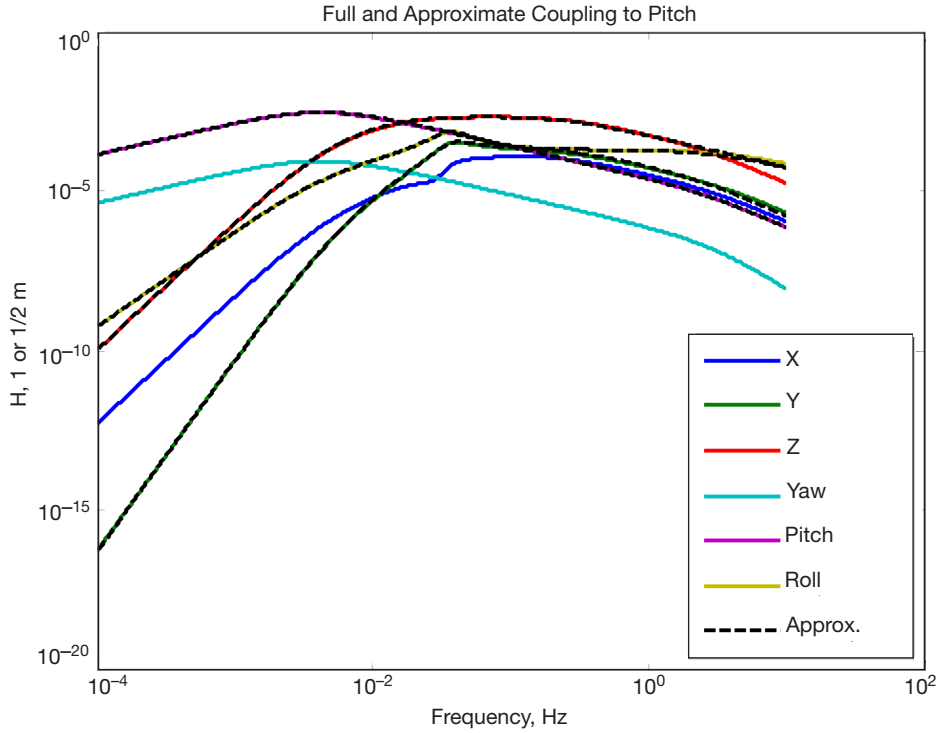

Figure 4. Transfer functions (magnitude) from spacecraft interface motion to platform pitch, calculated using the full 6 × 6 equation of motion and ("Approx.") using block-diagonal approximations

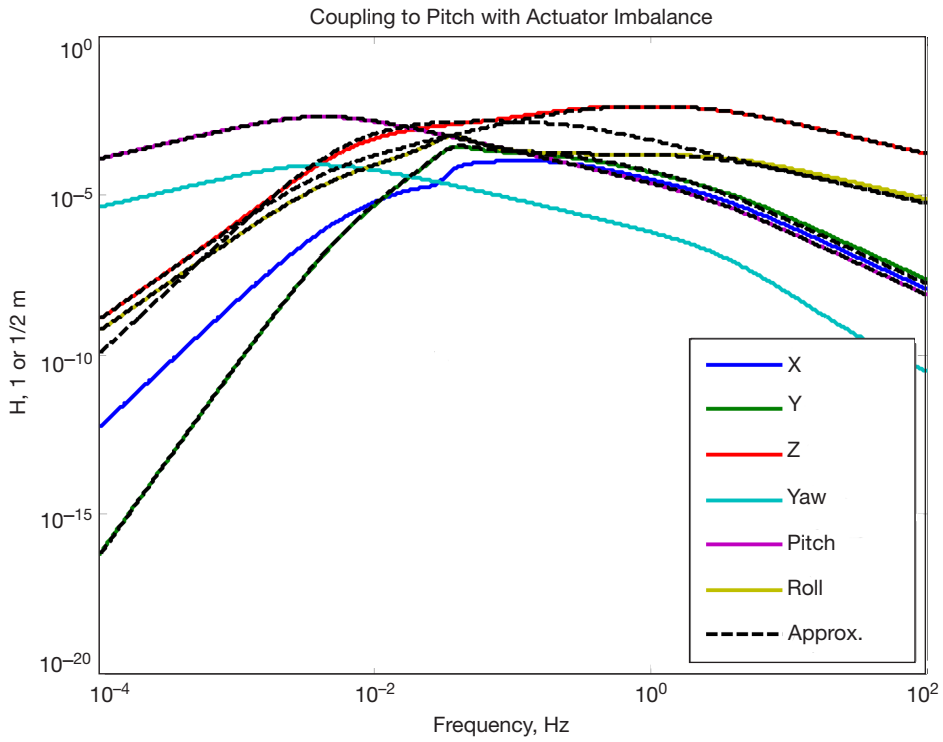

Figure 5. Transfer functions (magnitude) from spacecraft interface motion to platform pitch, for a 1 mm actuator transformation imbalance in response to Z force commands, calculated using the full 6 × 6 equation of motion and ("Approx.") using block-diagonal approximations.

This equation can be solved numerically and the results are shown in Figures 6 and 7. Noise in the pointing sensor results in an equal amount of pointing error below the unity-gain frequency of the external controller, as the controller causes the platform to follow the apparent motion corresponding to the pointing sensor noise. Pointing sensor noise, expected to be approximately 150 nrad/$Hz^{1/2}$, is the principal mechanism limiting the maximum allowable bandwidth in the two controllers (controlling pitch and yaw) that feed back from the pointing sensor.

Noise in the relative sensors is not expected to affect performance significantly. Sensors with noise of 1 nm/$Hz^{1/2}$ have been demonstrated at JPL;[9] over a 10-cm lever arm these have significantly lower noise equivalent angle than the expected pointing sensor noise, and the coupling from the relative sensors to pointing error is roughly two orders of magnitude smaller.

D. System Performance

System performance was assessed by defining a measure of performance, and the gains of the controllers were adjusted to meet a requirement taken to be 2 microradians of RMS pointing error, per axis.

[9] G. G. Ortiz, personal communication, Jet Propulsion Laboratory, Pasadena, California, n.d.

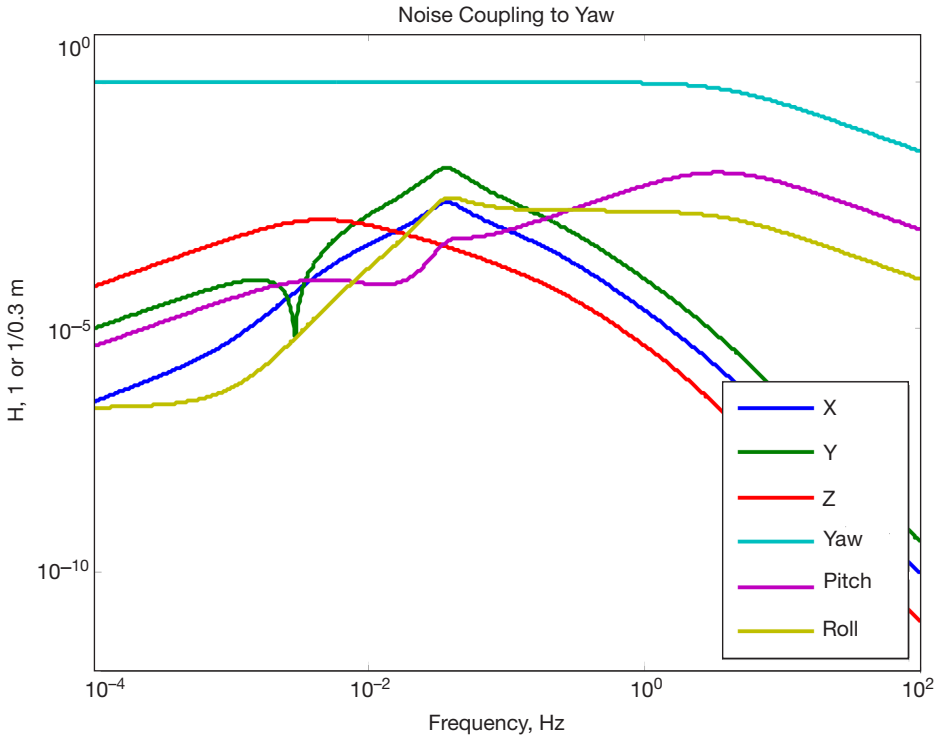

Figure 6. Transfer functions from sensor noise to yaw pointing error.

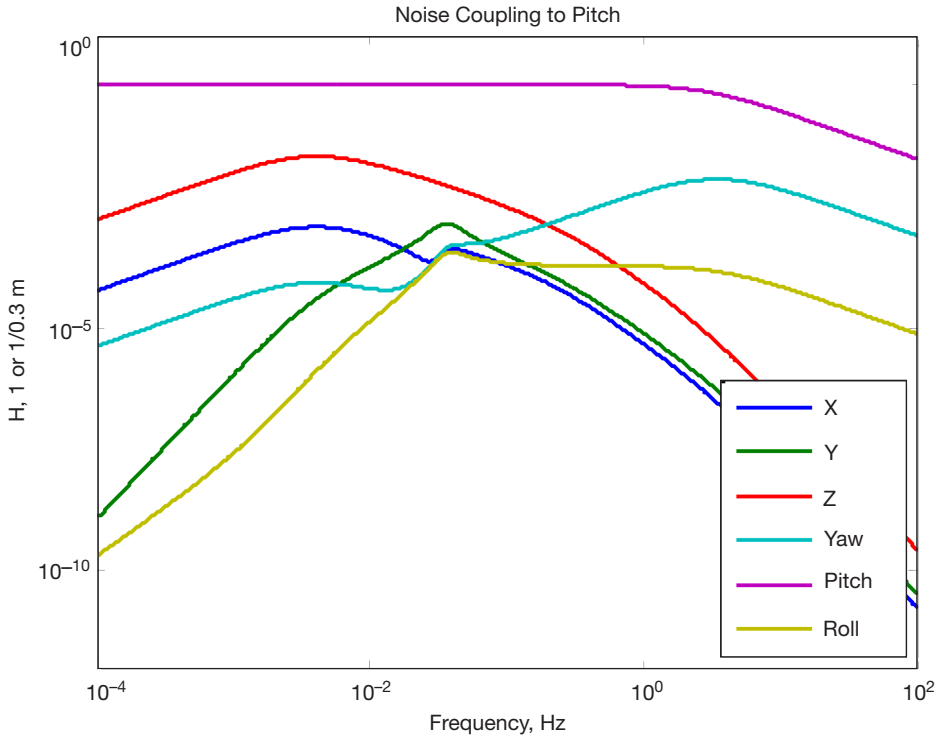

Figure 7. Transfer functions from sensor noise to pitch pointing error.

Pointing Error Calculation

The assumed rotational disturbance spectrum for each rotational degree of freedom was adapted from Burnside et al. [9] and is shown as "Rotational Disturbance" in Figure 8. The translational disturbance was assumed to be the rotational disturbance spectrum multiplied by the square of an assumed lever arm of 2 m, which is considered conservative. Because little was known about the cross spectra between these six spectra, or about the orientation of the platform at the spacecraft interface, the following approach was taken to estimate the total resulting platform pointing error. At each frequency, a matrix of transfer functions from the six degrees of freedom of spacecraft interface motion to the two degrees of freedom of pointing motion was calculated, and the magnitude of the largest transfer function element coupling rotation to pointing error was added to 2 m times the largest transfer function element coupling translation to pointing error, to account for the possibility of perfect correlation of the rotational and translational disturbances. This sum was then squared and multiplied by the rotational disturbance power spectrum of Figure 8, and integrated numerically over frequency to provide an RMS pointing error.

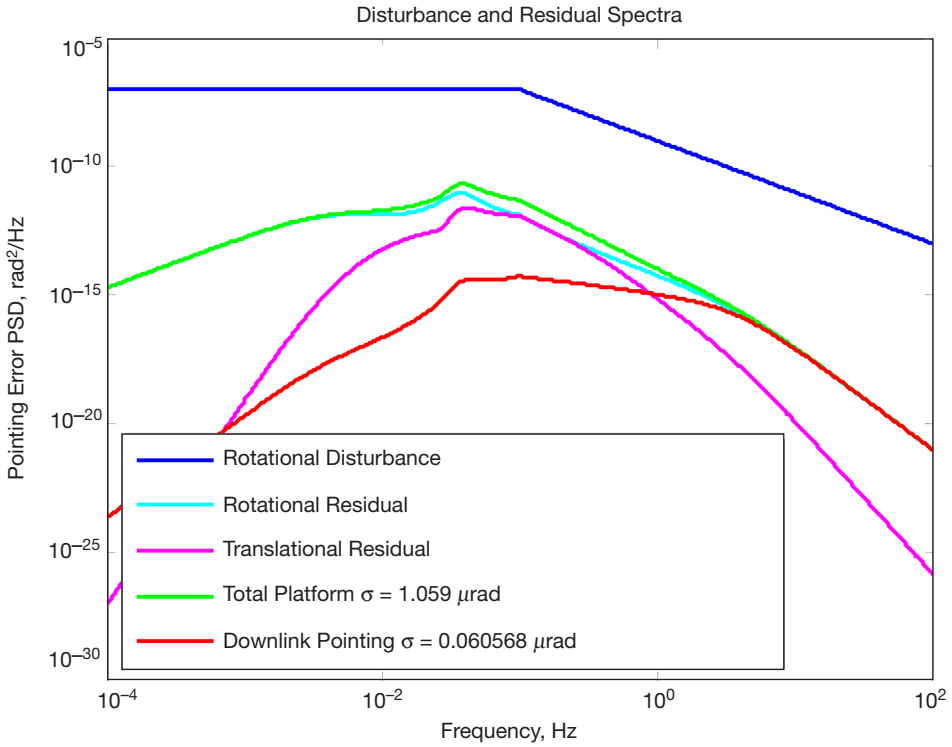

Figure 8. Power spectral density of the assumed spacecraft interface rotational motion ("Rotational Disturbance"), the resulting residual platform pointing error ("Total Platform"), the contributions to platform pointing errors from spacecraft interface rotational motion ("Rotational Residual"), and translational motion ("Translational Residual") and pointing error of a downlink beam ("Downlink Pointing").

Adjustment of Controller Gains

Adjustment of the controller gains followed an iterative process that converged quickly, guided by an understanding of the coupling mechanisms described above. The gains of the two loops feeding back from the pointing sensor were increased as much as possible without coupling in unacceptable sensor noise, and the gains of the local loops were increased to balance the coupling mechanisms that increase with increased gain against those that decrease with increased gain. Which mechanism produces the greatest contribution to the pointing error can be determined at any design point by temporarily turning off, in the model, one or more of the causes of coupling, e.g., making the spring constant matrix or the mass matrix diagonal.

This process was used to find a rough optimum in a few manual iterations for the system described here. Unity gain frequencies were: 3 Hz for the loops feeding back from the pointing sensor, 0.3 Hz for the local translation loops, and 0.03 Hz for the roll loop. The residual spacecraft disturbance predicted from this design is shown in Figure 8. The spectra of residual spacecraft interface translational and rotational motion, which together produce the "Total platform" pointing error of the platform, are shown separately. Also shown, for reference, is the downlink beam-pointing error, assuming that this error is attenuated by a cascaded loop controlling a beam-steering mirror, with a unity gain frequency of 3 Hz. Pointing error due to sensor noise is a separate error budget term and therefore not included in Figure 8.

III. Conclusion

The dynamics of a nearly free-floating vibration isolation system of the type being developed by JPL can be analyzed numerically with a simple model. Although in principle this 6×6 system could have rather complex behavior, when controlled with diagonal controllers the dominant transfer functions from spacecraft interface motion to platform motion are all well explained by mechanisms that involve only 2×2 or 3×3 cross-coupling. These mechanisms are easily understood and the insights they provide can readily be employed to design controllers meeting performance requirements.

References

[1] G. G. Ortiz, W. H. Farr, and V. Sannibale, "A Sub-Hertz, Low-Frequency Vibration Isolation Platform," *NASA Tech Briefs*, p. 18, January 2011.

[2] N. Pedreiro, A. C. Carrier, K. R. Lorell, D. E. Roth, G. Shelef, R. R. Clappier, and M. A. Gonzales, "Disturbance-Free Payload Concept Demonstration," AIAA Guidance, Navigation, and Control Conference and Exhibit, Monterey, California, August 5–8, 2002.

[3] N. Pedreiro, A. C. Carrier, K. R. Lorell, D. E. Roth, G. Shelef, R. R. Clappier, and M. A. Gonzales, "Disturbance-Free Payload Concept Demonstration," AIAA Guidance, Navigation, and Control Conference and Exhibit, Monterey, California, August 5–8, 2002.

[4] M. A. Gonzales, N. Pedreiro, D. E. Roth, K. Brookes, and B. W. Foster, "Unprecedented Vibration Isolation Demonstration Using the Disturbance-Free Payload Concept," AIAA Guidance, Navigation, and Control Conference and Exhibit, Providence, Rhode Island, August 16–19, 2004.

[5] L. Dewell, N. Pedreiro, C. Blaurock, K.-C. Liu, J. Alexander, and M. Levine, "Precision Telescope Pointing and Spacecraft Vibration Isolation for the Terrestrial Planet Finder," Coronagraph UV/Optical/IR Space Telescopes: Innovative Technologies and Concepts II, H. A. MacEwen, ed., Bellingham, Washington: *Proceedings of SPIE*, vol. 5899, August 18, 2005.

[6] T. L. Trankle, N. Pedreiro, and G. Andersen, "Disturbance-Free Payload Flight System Analysis and Simulation Methods," AIAA Guidance, Navigation, and Control Conference and Exhibit, San Francisco, California, August 15–18, 2005.

[7] N. Pedreiro, M. A. Gonzales, B. W. Foster, T. L. Trankle, and D. E. Roth, "Agile Disturbance-Free Payload," AIAA Guidance, Navigation, and Control Conference and Exhibit, San Francisco, California, August 15–18, 2005.

[8] N. Pedreiro, "Spacecraft Architecture for Disturbance-Free Payload," *Journal of Guidance, Control, and Dynamics*, vol. 26, no. 5, pp. 794–804, September–October 2003.

[9] J. W. Burnside, D. V. Murphy, F. K. Knight, and F. I. Khatri, "A Hybrid Stabilization Approach for Deep-Space Optical Communications Terminals," *Proceedings of the IEEE*, vol. 95, no. 10, pp. 2070–2081, October 2007.